All-Electric Aircraft Nose Wheel Steering System with Two Worm Gears

Zhang Ming[1*], *Li Chuang*[2], *Wu Xin*[3], *Zhu Yin*[3]

1. Key Laboratory of Fundamental Science for National Defense-Advanced Design Technology of Flight Vehicle, Nanjing University of Aeronautics & Astronautics, Nanjing 210016, P. R. China;
2. Shanghai Aircraft Design and Research Institute, Shanghai 201210, P. R. China;
3. Aviation Key Laboratory of Science and Technology on Aero Electromechanical System Integration, Nanjing 211106, P. R. China

(Received 18 May 2016; revised 20 September 2016; accepted 20 November 2016)

Abstract: As all-electric aircraft has many advantages, an aircraft nose wheel steering system would be developed to the all-electric direction. Concerning the control demand of the nose wheel steering system, based on the basic principles of nose wheel steering system and the design technique of mechanotronics, an all-electric aircraft nose wheel steering system, composed of a nose wheel steering mechanism of two worm gear and a control servo system of fly-by-wire with both steering and anti-shimmy functions is designed to meet the demand for operation control in the nose wheel steering system. Then, based on the LMS-AMESim software, the simulation model of the system is established to simulate the dynamics for the verification of its steering function. The simulation results indicate that the nose wheel steering system is reasonable, and can meet the requirements of the general project. Furthermore, the prototypes of the steering mechanism and control system are studied to validate the design, and the steering test bench is prepared to test the designed system. The test results, such as steer angle, rotate speed of motor are analyzed in details and compared with the theoretical results. The analysis and comparison results show that the design is reasonable and the property of the prototype can achieve the design objectives.

Key words: mechanotronics design; nose wheel steering system; all-electric; aircraft design; landing gear

CLC number: V261 **Document code**: A **Article ID**: 1005-1120(2018)01-0170-11

0 Introduction

More and more electric aircraft takes electric power system as its second power by using it to replace the original hydraulic, pneumatic and mechanical system[1,2]. As a result, it has the characteristics of simple structure, light weight, high reliability and high ratio of performance to price[3-5]. For the insurmountable and inherent defects of the hybrid system in current aircraft, the aircraft maintenance caused by such relevant systems accounts for more than 50% of the total aircraft maintenance[3]. Since all-electric system has high reliability, high maintainability, low security and operating cost, and many other inherent advantages, the nose wheel steering system would be developed in the all-electric direction[6]. The realization of all-electric aircraft depends on whether the aircraft function subsystem can be developed using the electric power as its power. The realization of the all-electric nose wheel steering system would perfect the overall aircraft performance, and speed up the all-electrification process of aircraft.

To date, the electric power systems used for flight control, environmental control, brake, fuel and engine starting system have been verified[6]. European scholars began to investigate the all-electric nose wheel steering system[7,8], they predict that the all-electrification would increase the

* Corresponding author, E-mail address: zhm6196@nuaa.edu.cn.

How to cite this article: Zhang Ming, Li Chuang, Wu Xin, et al. All-electric aircraft nose wheel steering system with two worm gears[J]. Trans. Nanjing Univ. Aero. Astro., 2018,35(1):170-180.
http://dx.doi.org/10.16356/j.1005-1120.2018.01.170

levels of reliability and availability significantly. Besides, the coordination and cooperation between the all-electric nose wheel steering system and automatic ground navigation system would increase the efficiency of air transport system. Refs. [9,10] describe the design and testing of a dual-lane electric drive for the operation of a prototype, electromechanically actuated, nose wheel steering system for a commercial aircraft. The drive features two fully independent motor controllers, each operating one half of a three-phase motor to produce an actuator capable of full operation in the event of an electrical fault.

Ref. [11] introduces the system architecture and redundance function principle and the design of peripheral interface circuit and the software of the digital skidpoof brake integrated controller. To prevent the similar redundant system occurring common fault avalanche damage, the dissimilar dual redundancy digital steering control box is designed in Ref. [12]. A nose wheel steering servo system composed of electromechanism actuator, controller and displacement sensor is introduced in Ref. [13]. The electromechanical actuator adopts the crew-slider-fork design to realize the requirement of miniaturization and high load.

For both civil aircraft and military aircraft, the realization of all-electric nose wheel steering system is significant to the improvement of ground operating performance.

An all-electric aircraft nose wheel steering system composed of a nose wheel steering mechanism of two worm gear and a control servo system of fly-by-wire having both steering and anti-shimmy function is designed here first. Then the simulation model of the system is established to simulate the dynamics for the verification of its steering function. Moreover, the prototypes of the steering mechanism and control system are built and tested to validate the design, and the steering test bench is prepared to test the work perform of the proposed system. The test results, such as steer angle, steer torque are analyzed in details and compared with the theoretical results.

1 Design of Nose Wheel Steering System

1.1 The overall scheme design

The nose wheel steering system belongs to the electromechanical actuator system, which is the general name for the position servo control system in aviation and aerospace, military, transportation, agricultural and industrial machinery and equipment, and controls the movement of its load directly or indirectly through controlling the operation of motor[14]. As shown in Fig. 1, it is composed of two main parts: The actuator module and the electric control unit.

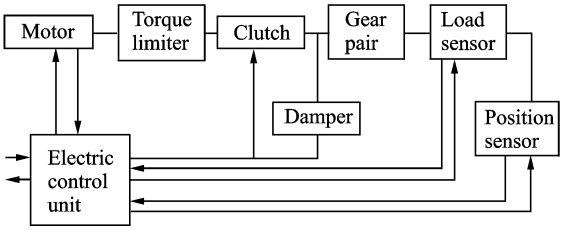

Fig. 1 Structure block of nose wheel steering system

The actuator module is responsible for converting electrical energy into mechanical energy and feeding back the mechanical transmission to control system. The diagram of the steering system is shown in Fig. 2, encompassing a motor, a torque limiter, a clutch, a reducer, a damper, a worm gear and sensors. In the process of aircraft steering on ground, the controller would firstly control the motor rotation according to the input signal. Then the motor would transmit its torque to the torque limiter, reducer and clutch successively. Consequently, the worm gear begins to rotate to realize the aircraft nose wheel steering. Its main components are described as follows:

Motor—According to the design require-

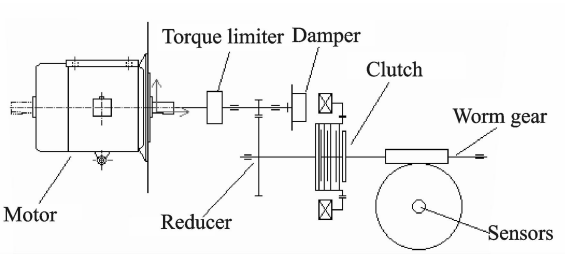

Fig. 2 Single redundant channel in steering system

ments of the aircraft nose wheel steering operating system, the friction torque loading in the nose wheel steering system is large, so the rare earth permanent magnet Direct Current (DC) motor with high power density and operating efficiency is selected by the system.

Clutch—The friction type clutch is selected by the system to control its status by control current. Once a fault occurs, the system would isolate the fault channel by controlling its clutch to disconnect.

Damper—To prevent the oscillation phenomenon, the damper is required to provide a damping for the nose wheel steering system. The damper does not work in system steering mode, however, it is activated by the main controller in system anti-shimmy mode.

Worm gear—The rated output torque provided by current motor is too small relative to the steering torque of the nose wheel steering system. As a result, larger transmission ratio should be provided by the machine transmission system. So the worm gear with inherent large transmission ratio is selected to be the system actuator.

The electronic control unit is responsible for position servo control and completing the closed loop of the nose wheel steering system, consisting of the main controller and the motor controller.

The main controller can realize the following three functions mainly:

(1) Be able to receive and process the sensor signals accurately, so as to achieve the servo control of the nose wheel steering system and load limiting of the torque limiter.

(2) Controlling the auxiliary equipment (such as clutch, damper and so on).

(3) Recording the fault information and detection data in fault points synchronously to support the next maintenance work.

The motor controller is mainly used for the amplification of control signal and control the steering direction and speed of the motor. The system uses DC pulse width modulation (PWM) converter to control the motor input voltage.

The assumption diagram of the controller is available, as shown in Fig. 4. As shown in Fig. 4, the main controller adopts similar dual redundancy design, and two channels communicate with each other through the dual port of random-access memory (RAM) and detect faults through cross supervision and self-supervision. In the process of nose wheel steering, the main controller would firstly judge whether the system is in a hand wheel operating mode or a pedal rudder operating mode based on digital signals. Then the main controller would acquire such analog signals as command signal, feedback signal and the aircraft ground speed, and thus conduct data processing by a certain control algorithm with reference to the control rate. Finally, the nose wheel steering servo control would be released.

To prevent the phenomenon of the non-coordination motion between the two worm gear of the system happening in the process of actual aircraft ground maneuver, the nose wheel steering system would feed back the worm gear steering angle in addition to the output torque of the two worm gear to the main controller. Then the difference between the system angle input and the worm gear wheel angle feedback, and the difference between the output torque of the two worm gear would be carried on a certain processing to be the output of the main controller to control the motor through adjusting the relationship between the two differences to ensure the steering process accurate and fluent. Fig. 3 shows the cross-supervision and self-supervision functions.

1.2 Main design parameters of the transmission component

Based on the aircraft nose wheel steering system design index, under 24 V DC, the maximum steering torque, the maximum steering angle, and the maximum steering speed provided by the nose wheel steering system are set as 1 000 N·m, 80° and 20 °/s, respectively.

Considering the commonly used motor speed, reducer transmission ratio range and worm gear transmission ratio range, refer to the rele-

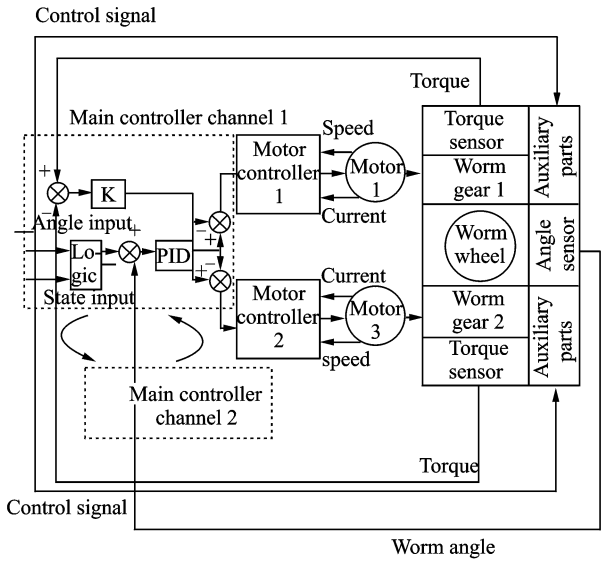

Fig. 3 Design diagram of the controller

vant design handbook, the motor model, the transmission ratio of the reducer and worm gear can be obtained, respectively. Then the main transmission components of the nose wheel steering system are designed concretely according to the handbook of mechanical and electric design. Finally, the main parameters of these transmission components are obtained, as shown in Table 1.

Table 1 Main parameters of transmission component

Parameter	Value	Parameter	Value
Motor rated power/ kW	0.259	Worm gear number of teeth	28
Motor rated torque/ (N·m)	0.405	Worm gear module	6.3
Motor rated speed/ ($r \cdot min^{-1}$)	5 990	Worm gear diameter coefficient	7.936
Electro mechanic time constant/ ms	3.75	Worm gear center distance/ mm	115
Reducer drive ratio	74	Worm diameter/ mm	50
Worm gear drive ratio	28	Worm wheel diameter/ mm	176.4
Worm gear tooth profile angle/(°)	20	Worm gear end efficiency	0.815
Coefficient of top clearance	0.2	Worm material	40cr
Addendum factor	1.0	Worm wheel material	ZCuSn6 Pb6Zn3
Number of threads	1	Worm gear efficiency	0.6

1.3 Preliminary design of damper

The schematic of damper is shown in Fig. 4. The electromagnetic damper has the inner magnetic type discrete structure. Its stator is composed of the internal stator and outer stator. The rare earth permanent magnet is in the inner stator, and the outer stator is made of the material with good magnetic conductivity. The rotor cup is located between the inner stator and the outer stator. Being induced to rotate by the motor, the metal rotor cup would cut the stator magnetic field, and thereby induce eddy current interacting with the stator magnetic field to produce damping torque.

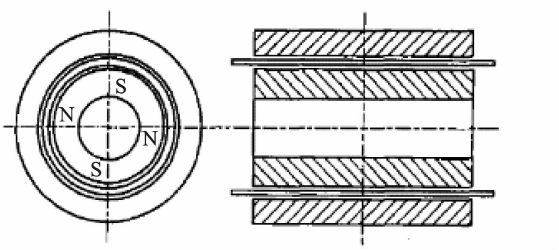

Fig. 4 Schematic of damper

The relationship between the damping torque T and the rotor rotational speed n in the damper is as follows[15]

$$T=\pi^2 B^2 \delta \cdot lp \frac{n\varepsilon}{60\rho} DRe \frac{-1}{k^2+\mathrm{i}\omega\alpha} \times \left[\frac{\tanh(\beta l/2)}{\beta l/2\left(1+(k/\beta)\tanh(\beta l/2)\tanh\left[k\cdot\left(\frac{L-l}{2}\right)\right]\right)}-1\right] \tag{1}$$

where B represents the magnetic induction intensity, δ the gap length, l the length of stator, ε the rotor cup thickness, D the rotor diameter, k the ratio of π/τ, τ the electrode gap, p the number of pole-pairs, ρ the rotor resistance, L the length of the rotor cup, ω the angular frequency, and $\alpha=\mu_0\varepsilon/\rho\delta$, $\beta=k^2+\mathrm{i}\omega\alpha$.

The functional relationship between the damping torque and the rotor rotational speed is nonlinear, so the damper with large value of p/D is selected in this system for simplifying the relationship into linear function. The ratio between the torque and speed is the damping coefficient K.

$$K = \pi^2 B^2 \delta L \frac{\varepsilon}{240 p \rho} D^3 r \quad (2)$$

where r is the correction factor.

Considering the ground impact load and tire aligning stiffness in the process of aircraft taxiing, landing gear's moment of inertia and the design requirements of nose wheel steering system, the damping coefficient can be obtained by establishing simulation model to simulate the anti-shimmy process of the nose wheel under the ground impact load. Finally, parameters of the damper can be obtained accordingly.

1.4 Layout and installation design of the system

Based on the main parameters of the system and the related design handbook, the layout and installation design of the system can be completed. As shown in Figs. 5,6, being the diagram of the nose wheel steering system installed on landing gear and the transverse sectional view of the nose wheel steering system. In the nose landing gear of aircraft, the first housing of the nose wheel steering system is fixed in the strut cylinder sleeve through screws. On the left side of the nose wheel steering system, the first motor and the first reducer located within the second housing, the first clutch is fixed in the second housing by screws and connected with the first reducer through the general flat key. Besides, the first motor and the first reducer fixed axially through the second housing. The first housing and second housing are fixed by bolt connection. One end of the first worm gear in first housing is connected with the first clutch through general flat key, and the other end is axially fixed through the first tapered roller bearing and the first end cap. The first cylindrical roller bearing and the first tapered roller bearing are installed on both ends of the first worm gear, respectively. The first cylindrical roller bearing is axially fixed through the shaft shoulder on the first worm and the first circlip for hole. The first tapered roller bearing is axially fixed through the first nut and the shaft shoulder on the first worm. The first end cap is fixedly connected with the first housing through bolts and contacts with the outer ring of the first tapered roller bearing. The installation of the right side nose wheel steering system is the same with the left side's.

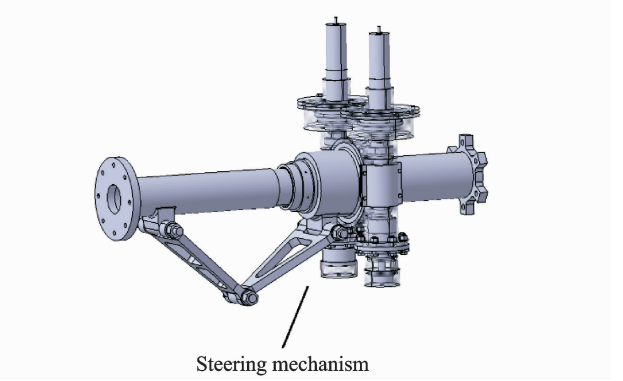

Fig. 5 Nose wheel steering system installed on landing gear

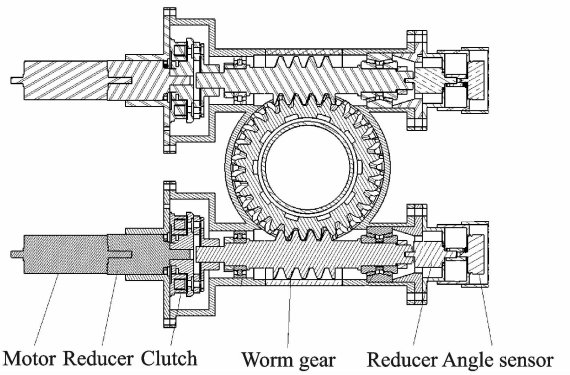

Fig. 6 Transverse sectional view of the nose wheel steering system

2 Simulation of All-electric Nose Wheel Steering System

2.1 Construction of all-electric nose wheel simulation model

Based on the afore-mentioned nose wheel steering system and the speed governing system of DC motor, the simulation model of all-electric nose wheel steering system has been established by using the AMESim software, as shown in Fig. 7.

The motor module of this model is created according to the speed governing system of DC motor, and is encapsulated. The clutch model consists of a piecewise linear function module and a free-rotation Coulomb friction module, which functions as a clutch and a torque limiter. Meanwhile, the clutch also sets a maximum Coulomb

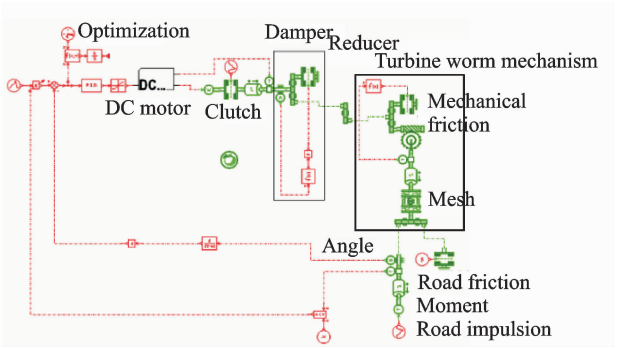

Fig. 7 Simulation model of nose wheel steering system

friction torque for the motor.

The damper module in this model is comprised of an angular velocity sensor, a coulomb friction module with one end fixed, a coupling module, and a function module. So the damper can become operational. The reducer module of AMESim is suitable for the reducer in this model. The reduction ratio should be chosen as 74.

The turbine worm mechanism module is made up of a running clearance module, a moment of inertia module, a moment sensor module, a turbine worm module, a Coulomb friction module with one end fixed, a coupling module, and one function module. Thus, the entire module is operational. Running clearance module is added to the model and grants better accuracy because clearance exists in practical situations inevitably.

2.2 Optimization on the model and relevant analysis

In practical engineering applications, PID parameters are adjusted manually so as to guarantee the dynamic performance of the control system. However, it is usually not the ideal state for the dynamic performance. Currently the performance index, integrated time and absolute error (ITAE), has been widely used to assess the dynamic performance of a system, which equals to time multiplied by absolute value of error and integrated over time. The index ITAE poses both practical and selective in engineering applications. The ITAE module adopted in the simulation system is shown in Fig. 8.

Considering nose wheel steering system in

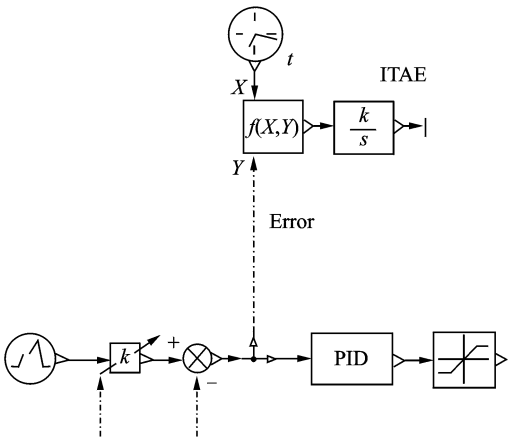

Fig. 8 ITAE module of the nose wheel steering system

the steering state, where electromagnetic damper is disabled and landing impact load is ignored. Ground load is 1 000 N · m fixed damping torque. In the beginning, nose wheel is situated in the middle. After one second, signal the nose wheel to ensure that the wheel rotates at 20°/s in the direction of one side until it reaches its extreme position. Afterwards, the wheel keeps working for a while. Finally, the wheel rotates back to its initial position at the same rate.

For achieving optimized PID parameters, proportionality coefficient, integral coefficient, and differential coefficient are selected as optimizing variables. The ITAE is used as the target function of optimization. By means of non-linear programming by quadratic Lagrangian (NLPQL) algorithm module integrated in the AMESim software, the minimum value of target function becomes accessible. Finally, optimal PID parameters are available: 207 as the proportionality coefficient, 0.002 as the integral coefficient and 29.5 as the differential coefficient. Two curves of nose wheel yaw angle over time are concluded by batching and comparing with the manually adjusted results.

As shown in Fig. 9, manually-adjusted curve's yaw angle overshoot is 2.7% with a small amount of settling time. Thus it meets the requirements of practical engineering. Yet after performing the optimization on PID parameters, overshoot of yaw angle output reaches almost ze-

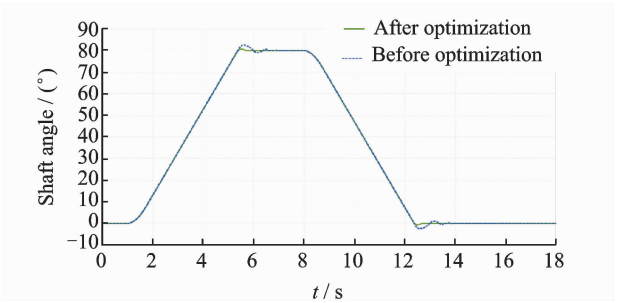

Fig. 9 Manually adjusted curve and optimized curve of yaw angle over time

ro, settling time is also reduced by 0.5 s. The dynamic performance of the entire system is considerably improved.

Fig. 10 demonstrates curves of optimized nose wheel steering input and output over time. It is evident that output curve lags behind the input curve all along the process. The reason for this situation is that during practical application, rotor's moment of inertia along with the clearance and friction in the motor lead to a small period of time when the motor reaches its rated speed from state of rest. Afterwards the system input maintains the maximum rotation speed until reaching extreme position, so input signal is not able to keep up with output signal, which is fairly normal. The output curve has the same trend as the input curve, where the lag is no more than 0.5 s. This symbolizes a remarkable follow performance that fulfills actual engineering practice.

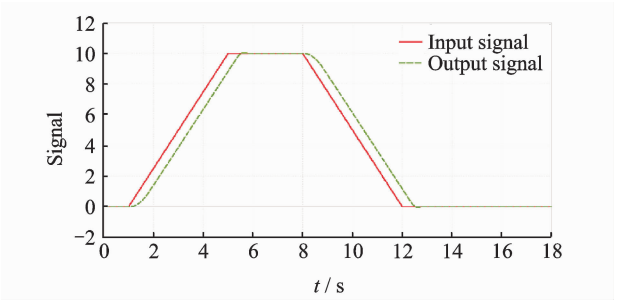

Fig. 10 Input and output curves over time of nose wheel steering system

During the steering process, load simulation system applies consistent load. Load is applied by the mechanism installed on the end of the steering system which generates friction against steering. Therefore, friction maintains an invariant value

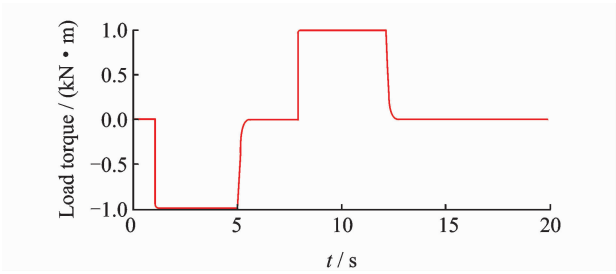

Fig. 11 Simulated load torque

just as shown in Fig. 11.

The DC motor's torque and rotating speed curves over time are shown in Fig. 12. It is obvious that it takes 0.5 for the motor to accelerate to rated speed 5 990 r/min from zero during the steering process, which is why input curve lags behind output curve. Since then motor maintains its speed until nose wheel reaches the yaw angle of 80°, where the steering system, as well as the motor, cease to function. In the process of the nose wheel returning to its initial position, the rotating speed of motor remains the same value as previous but in opposite direction. The working torque of the motor during steering is 0.395 N • m, which is similar to rated torque. This guarantees long time of work and exploiting performance better.

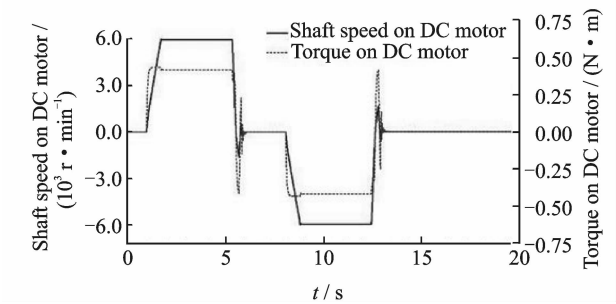

Fig. 12 DC motor's torque and rotating speed curves over time

Since the simulation process is relatively ideal, two servo motors share the same status of motion when their parameters are configured identically. Therefore, one parameter is modified manually in order to test the speed configuring module.

By comparing Fig. 13 and Fig. 14, the following conclusion is drawn: Before speed configu-

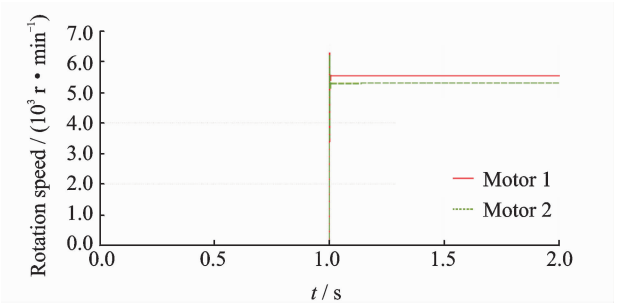

Fig. 13 Motor rotate speed before configuration

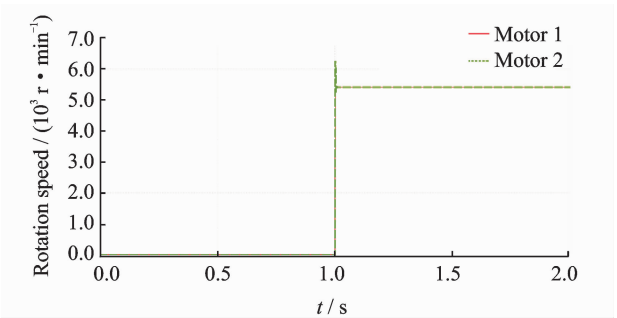

Fig. 14 Motor rotate speed after configuration

ring module works, two motors differ in speed. While the module is operational, two motors remain almost the same rotate speed.

3 Test Verification

The main objective of nose gear steering mechanism test verification is to analyze the feasibility of entire steering mechanism design and the accuracy of control system. The experiment requires the entire system to simulate the actual steering process, which calls for the whole nose gear entity and its control system. Moreover, the steering test verification system must provide steering angle, rotate speed of motor and commands from control system during steering process for further analysis on the feasibility.

3.1 Basic theory and control system of the experiment

Landing gear steering experiment system consists of two systems: control system and measure system. The control system exerts control over the steering system while the measure system gauges rotate speed of nose gear and motor, as well as feeds all the data back to the control system. Thus it is guaranteed that steering mechanism stays the same working condition in practice. To make it convenient to install and configure the entire landing gear, one end of the mechanism is fixed, while the other end is free for further load simulation as shown in Fig. 15.

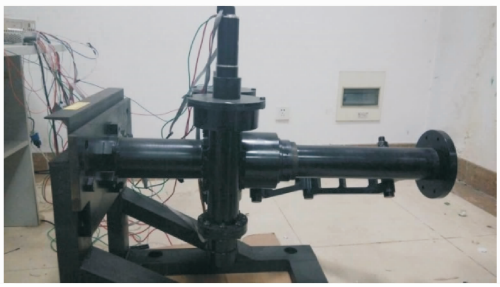

Fig. 15 Image of the steering mechanism

(1) Controller

The control system has been integrated to a control box whose user interface can be easily modified and designed. DSP control unit is applied for the experiment, which grants swift process and accurate control.

Fig. 16 DSP control unit

DSP control unit integrates assorted sensors for switching anti-shimmy modes, measuring displacements of steering system and load applied on the landing gear, along with modules connecting servo motors. As a result, clutching device, servo motor and sensors have to be connected to the control unit accordingly.

Fig. 17 shows the wire map of control unit, components of the steering system are linked to the DSP control unit respectively. Corresponding components can be manipulated by internal commands from the control system, thus the steering

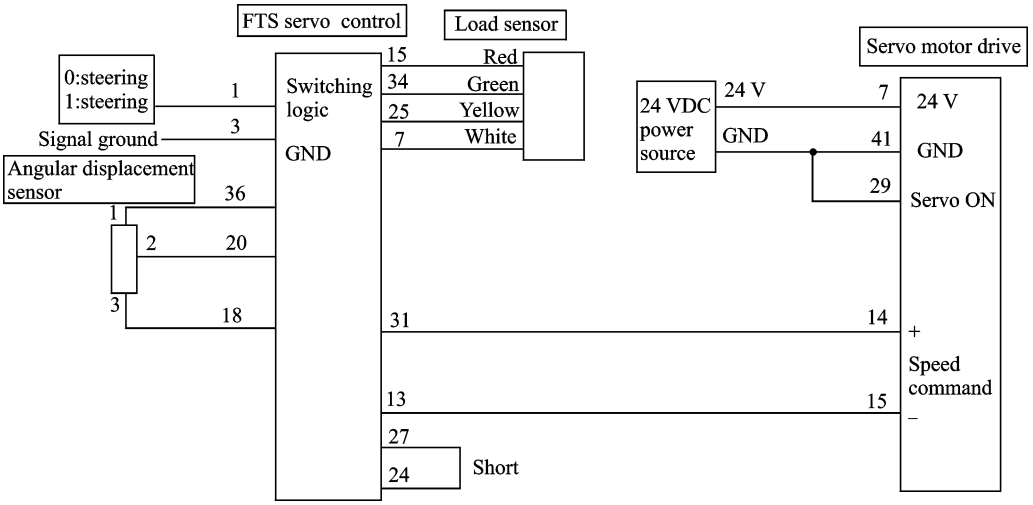

Fig. 17 Wire map of DSP control unit loop

mechanism is able to function properly.

(2) Control method of servo motor

There are three methods for servo motor control strategies: Torque control, position control and speed control. Speed control strategy is adopted due to the experiment requirement that speed has to be maintained during test. Analogue parameters can be harnessed to control the rotate speed. Furthermore, speed control strategy is capable of accurate positioning with the outer loop PID control along with upper control device, which reduces error during transmission and adds to the accuracy of positioning for the whole system.

Control strategy for servo motor is displayed as Fig. 18. By means of outputting correspondent analogue signals to manipulate rotate speed of motor. Meanwhile, analogue offset and auxiliary input signals to ensure the precision of any command.

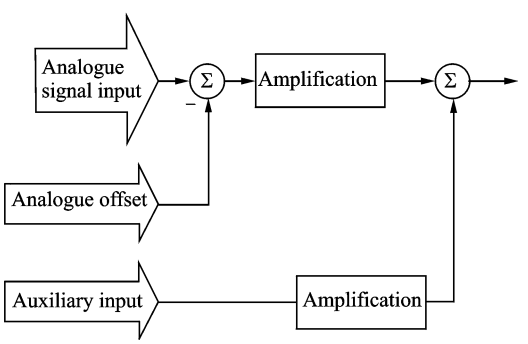

Fig. 18 Control theory of motor

3.2 Results and analysis of the experiment

Real-time monitoring of rotate speed of servo motor has been performed by sensors during rotation. The rotate speed has been recorded and manipulated by presetting DSP control signals.

Recording of working status of servo motor is conducted by Motion Monitor software as Fig. 19 presents. Both actual rotate speed and preset speed are accumulated, along with current fluctuation and actual displacement of motor.

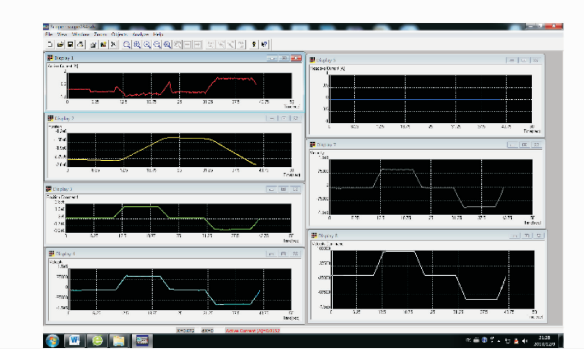

Fig. 19 Recorded data

Fig. 20 represents the command of speed and control signal. It is apparent that DSP voltage keeps up with the operation of motor consistently. In the beginning servo motor holds still, when DSP voltage rises, Servo motor's rotate speed increases proportionally. Motor's rotate speed follows voltage very well, therefore DSP control unit plays an outstanding role for the experiment.

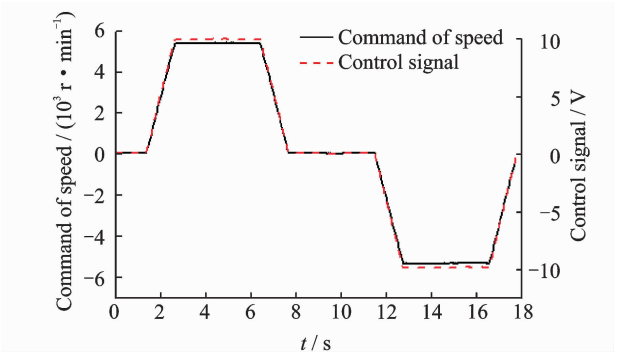

Fig. 20 Command speed and control signal

Fig. 21 shows a good consistency between command speed and actual speed, which indicates a proper set of parameters.

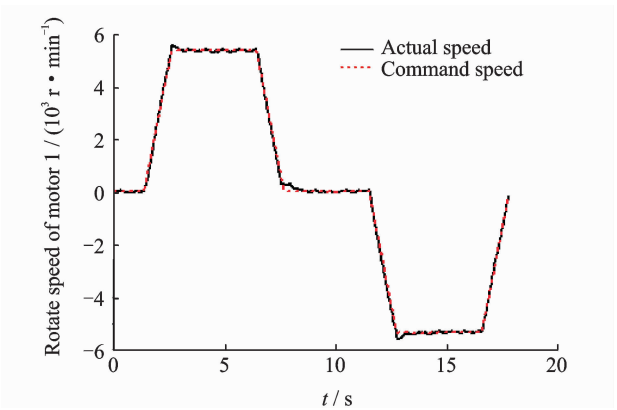

Fig. 21 Command speed and actual rotate speed

In the process of steering, respective measurements are applied to the servo motors as shown in Fig. 22. Two motors remain basically the same rotate speed. As a result, it is evident that excess energy dissipation of the system caused by nonsynchronous movement of two worms.

Fig. 23 shows the displacement curve of steering mechanism. When given proper input

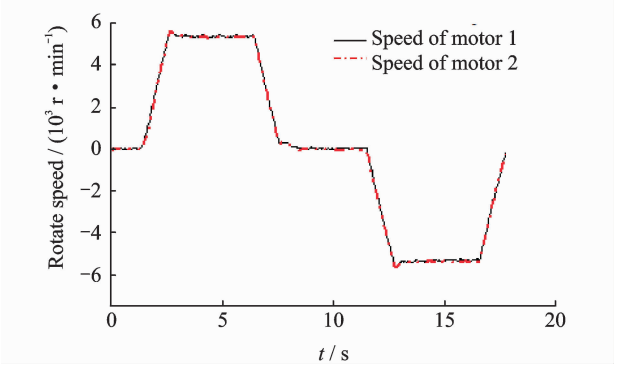

Fig. 22 Rotate speed of two motors

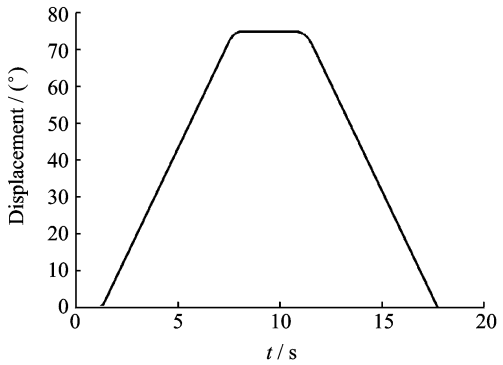

Fig. 23 Rotation displacement of servo motor

signals, the mechanism starts working until reaches the designated angle, where the system ceases to function. Afterwards, steering mechanism returns to its initial position on corresponding command.

4 Conclusions

The design method of all-electric nose wheel steering system is addressed, including the machanical design and control strategy design. Then the simulation method is used to determine the design parameters and the prototype test is used to verify the design reasonableness.

(1) Two DC motors, two worms and one worm wheel are designed to improve the steering torque. Nose wheel steering system under 24 V DC can provide 1 000 N • m steering torque, 80° steer angle and 20 °/s steering angular velocity.

(2) The main controller feeds back the worm gear steering angle in addition to the output torque of the two worm gear to make them rotate synchronously. The simulation annlysis is conducted to verify the property. PID parameters are adjusted to improve the steering performance.

(3) The prototypes of the steering mechanism and control system are researched to validate the design and the steering test bench is prepared to test the system working. The test results, such as steer angle, rotation speed of motor are analyzed in details and compared with the theoretical results. The test results indicate that all-electric nose wheel steering system with two worm gears is qualified for an intact steering mecha-

nism.

Acknowledgement

This work was supported partly by the Aeronautical Science Foundation of China (No. 20142852025).

References:

[1] LIU Ming, HUANG Chunzhou, Li Qin. Subsystems development on more-electric aircraft[J]. Astronautical Science and Technology, 2005(6): 10-13. (in Chinese)

[2] ZHU Xinyu, PENG Weidong. The application of more-electric aircraft and its technology[J]. Journal of Civil Aviation Flight University of China, 2007,18(6):8-11. (in Chinese)

[3] JONES R I. The more electric aircraft-assessing the benefits[J]. Journal of Aerospace Engineering, 2002, 216(5):259-269.

[4] LESTER F. Beyond the more electric aircraft[J]. Aerospace America, 2005, 9:35-40.

[5] WEIMER J. Past, present & future of aircraft electrical power systems: AIAA 2001-1147[R]. USA: AIAA, 2001: 1-9.

[6] YU Liming. The improvement and development in the technical analysis of all-electric aircraft[J]. Aircraft Design, 1999, 9(3):1-2. (in Chinese)

[7] DRESS. Distributed and redundant electro-mechanical nose wheel steering system[R]. Paris Air Show: DRESS Early Achievements Presentation, 2009.

[8] LISCOUET J, MARE C, BUDINGER M. An integrated methodology for the preliminary design of highly reliable electromechanical actuators: Search for architecture solutions[J]. Aerospace Science and Technology, 2012, 22(1):9-18.

[9] BENNETT J W. Fault tolerant electromechanical actuators for aircraft[D]. England: Newcastle University, 2010.

[10] BENNETT J W, MECROW B C, ATKINSON D J, et al. A fault tolerant electric drive for an aircraft nose wheel steering actuator[J]. IET Electrical Systems in Transportation, 2011, 1(3):117-125.

[11] HUI Xiaoqiang, ZHOU Bo, ZHANG Lei, et al. Design of digital skidproof brake integrated controller in airplane [J]. Aeronautical Computing Technique, 2010, 40(5):126-130. (in Chinese)

[12] ZHAN Xiang. A design of dissimilar dual redundancy digital steering control box based on FPGA and DSP[J]. Journal of Xihua University: Natural Science, 2015, 34(4): 32-36. (in Chinese)

[13] WANG Aping, WU Hao, CAO Sijia, et al. Research on a miniaturized and high load nose wheel steering servo system for aircraft[J]. Aviation Precision Manufacturing Technology, 2017, 53(2):38-41. (in Chinese)

[14] GUO Hong, XING Wei. Development of electromechanical Actuators[J]. Acta Aeronoutica et Astronautica Sinica, 2007, 28(3):620-627. (in Chinese)

[15] WANG Youlin, LIU Jinglin. Designing electromagnetic damper used in space rendezvous[J]. Journal of Northwestern Polytechnical University, 2006, 24(3): 358-362. (in Chinese)

Dr. **Zhang Ming** received the Ph. D. degree in aircraft design from Nanjing University of Aeronautics and Astronautics (NUAA), Nanjing, China, in 2009. From 2009 to present, he has been with the College of Aerospace Engineering, NUAA, where he is currently an associate professor of Key Laboratory of Fundamental Science for National Defense-Advanced Design Technology of Flight Vehicle (NUAA). His research has focused on landing gear system design, aircraft system dynamics.

Mr. **Li Chuang** received the B. Sc. degree in aircraft design from NUAA, Nanjing, China, in 2015. From 2015 to present, he has been with the Shanghai Aircraft Design and Research Institute, Shanghai, China. His research has focused on landing gear system design, aircraft system dynamics.

Prof. **Wu Xin** received his B. Sc. degree from NUAA, Nanjing, China, in 1993. He has been a special technology expert of AVIC, works in the Institute of Aviation Accessories of China. His research has focused on the development of aircraft hydraulic control system and hydraulic accessories. He had many experiences in the development and application of Nose Wheel Steering Systems (NWSS), and conducted or participated in the development of nearly 20 type NWSS.

Ms. **Zhu Ying** received her B. Sc. degree in hydraulic system design from Beihang University, Beijing, China, in 1985. From July 1985 to present, she has been with the Nanjing Engineering Institute of Aircraft Systems / Aviation Key Laboratory of Science and Technology on Aero Electromechanical System Integration. Her research has focused on hydraulic system of aircraft.

(Production Editor: Zhang Tong)